

Investigation on the photoproduction of bottom-charmed baryon within NRQCD

Juan-Juan Niu^{1*} and Hong-Hao Ma^{2,1†}

¹ Department of Physics, Guangxi Normal University,
Guilin 541004, People's Republic of China and

² Instituto de Física Teórica, Universidade Estadual Paulista,
Rua Dr. Bento Teobaldo Ferraz, 271- Bloco II, 01140-070 São Paulo, SP, Brazil
(Dated: January 29, 2026)

We present a further theoretical study of the orbital P -wave bottom-charmed baryon within the framework of nonrelativistic QCD (NRQCD), considering both the direct photoproduction channel $\gamma + \gamma \rightarrow \Xi_{bc} + \bar{c} + \bar{b}$ and the resolved photoproduction channel $\gamma + g \rightarrow \Xi_{bc} + \bar{c} + \bar{b}$. At future linear colliders, ILC and CLIC, the initial photons can be emitted from the laser back-scattering (LBS) and then the parton gluon can be emitted from the photon. The formation of Ξ_{bc} can be modeled in two-step: a compact diquark state $\langle bc \rangle[n]$ is formed first and subsequently captures a light quark from the vacuum to hadronize into the baryon Ξ_{bc} . The color and spin quantum number $[n]$ of $\langle bc \rangle$ -diquark can be $[^3S_1]_{\bar{3}/6}$, $[^1S_0]_{\bar{3}/6}$, $[^1P_1]_{\bar{3}/6}$ or $[^3P_J]_{\bar{3}/6}$ with $J = 0, 1, 2$. Based on the collision energies and design luminosity of ILC and CLIC, the cross sections, the differential distributions and the estimated produced events of Ξ_{bc} baryon have been analyzed. The results show that the contribution of the orbital excited P -wave Ξ_{bc} baryon can reach 7%-9% of the S -wave, providing a non-negligible contributions.

I. INTRODUCTION

Since the discovery of doubly charmed baryon Ξ_{cc}^{++} by LHCb Collaboration in 2017 [1–3], the quark model [4–6] has achieved a successful verification, while also presenting new challenges. It predicted the existence of bottom-charmed baryons, which consist of two different heavy quarks (b and c) and a light quark (u , d or s) in multiplets. Due to its heavy mass and the need for the both b and c component quarks, compared to the doubly charmed baryons, its production cross-section is smaller. The LHCb Collaboration using proton-proton collision data performed the first search for the $\Xi_{bc}^+(bcu)$, $\Xi_{bc}^0(bcd)$ and $\Omega_{bc}^0(bcs)$ baryon through the decay channel $\Xi_{bc}^+ \rightarrow J/\psi \Xi_c^+$, $\Xi_{bc}^0 \rightarrow D^0 p K^-$, and $\Xi_{bc}^0/\Omega_{bc}^0 \rightarrow \Xi_c^+/\Lambda_c^+ \pi^-$ [7–9]. However, these bottom-charmed baryons have not yet been confirmed their existence through experiments to date. Meanwhile, focus on the mass, lifetime, production mechanisms and decay properties of Ξ_{bc} (here, the light quark is not explicitly identified) and their excited states, a series of in-depth theoretical studies were carried out using theoretical potential models and phenomenology [10–19]. The study of these hadrons plays an indispensable role in understanding the Quantum Chromodynamics (QCD) theory, revealing the interaction between quarks and gluons, and exploring the structure of baryon.

* niujj@gxnu.edu.cn

† honghao.ma@unesp.br, corresponding author

With the improvement of the collision energy and luminosity in high-energy physics experiments, the feasibility of discovering the bottom-charmed baryon has been greatly enhanced. At the same time, more precise theoretical calculation results are required for the guidance of experimental exploration. In the early stages, a large number of theoretical predictions focused on the production mechanisms of doubly heavy baryons Ξ_{cc} , Ξ_{bc} , and Ξ_{bb} in S -wave on multiple platforms, including direct production at hadron colliders [20–31], electron-positron colliders[32–35], $\gamma\gamma$ [20, 36–38] collision, ep collision [20, 39, 40], heavy-ion colliders[26, 41], as well as the indirect production through top quark decays [42], Higgs [43], W^+ [44], and Z^0 [45] bosons decay. Subsequently, research on the production mechanism of excited P -wave doubly heavy baryons has been carried out successively [44, 46–49]. The results show that the contributions of doubly heavy baryon in P -wave can not negligible, reaching several percent, and it is worthy of further in-depth study. Therefore, at e^+e^- colliders, the photoproduction of doubly heavy baryons Ξ_{bc} in P -wave can be conducted.

Regarding the photoproduction of doubly heavy baryons Ξ_{bc} at e^+e^- colliders, it is typically a direct process $\gamma+\gamma \rightarrow \Xi_{bc}+\bar{c}+\bar{b}$ and the resolved channel $\gamma+g \rightarrow \Xi_{bc}+\bar{c}+\bar{b}$ [50]. The initial γ can be emitted either form the bremsstrahlung process and its energy distribution can be well delineated within the Weizäcker-Williams approximation (WWA) [51], or from the process of laser back-scattering (LBS) of e^+e^- at future linear colliders, ILC and CLIC [52, 53]. However, the photons from these two sources have different trends. The photon spectrum of LBS shows an upward trend, while that of WWA shows a logarithmic decline trend [38, 54]. Future e^+e^- colliders, such as FCC-ee [55], CEPC [56, 57], ILC [52, 58] and CLIC [53] has provided a very favorable experimental platform for the search for bottom-charmed baryons. Especially at ILC and CLIC, the contribution of resolved photoproduction channel ($\gamma+g$) of Ξ_{bc} is significant, which is attributed to the LBS photon [59–63]. And the contribution from double resolved photoproduction channel is usually very small and can be disregarded. After the LBS photon undergoes a process of resolution, its partons (γ , g , u , d , s) will participate in the subsequent strong interaction, resulting in a high-energy process that must involve final-state particles b and c quarks. However, for the production of bottom-charmed Ξ_{bc} baryon, the key lies in the non-perturbative hadronization process.

Non-relativistic quantum chromodynamics (NRQCD) [64] provides a good theoretical framework to effectively solve such production problems [65]. Within the framework of NRQCD, the production of hadron can be factorized into two parts: the perturbative region and the non-perturbative region. Firstly, in the hard process, the free final-state particles b and c quarks are perturbatively produced into a diquark with a distinct quantum state $\langle bc \rangle[n]$, and then this intermediate diquark state non-perturbatively transitions to the bottom-charmed baryon Ξ_{bc} , this transition process can be described by the wave function at the origin with potential models. The spin and color quantum number $[n]$ of $\langle bc \rangle$ -diquark can be $[^1S_0]_{\bar{\mathbf{3}}/\mathbf{6}}$, $[^3S_1]_{\bar{\mathbf{3}}/\mathbf{6}}$, $[^1P_1]_{\bar{\mathbf{3}}/\mathbf{6}}$, and $[^3P_J]_{\bar{\mathbf{3}}/\mathbf{6}}$ ($J=0, 1, 2$). These diquark states respectively correspond to 1S_0 and 3S_1 configurations of S -wave, 1P_1 and 3P_J configurations for excited P -wave. $\bar{\mathbf{3}}$ and $\mathbf{6}$ are the color quantum number of $\langle bc \rangle$ -diquark, representing the color anti-triplet state and sextuplet state for the decomposition of $SU(3)_c$ color group $\mathbf{3} \otimes \mathbf{3} = \bar{\mathbf{3}} \oplus \mathbf{6}$. The corresponding hadronization of these states can be expressed using the long-distance matrix elements (LDMEs). In the final hard process, that is, the short-distance coefficient, the energy dependence of the cross section for the photoproduction of Ξ_{bc} in S -wave initially increases rapidly, reaches its maximum at around 90 GeV, and then decreases steadily [59]. Here, in order to give a comprehensive comparison and analysis, the cross section for the photoproduction of the ground and excited states Ξ_{bc} baryons are investigated at ILC and

CLIC with collision energy $\sqrt{s} = 250, 500, 1000$ GeV, respectively.

In this work, the photoproduction of bottom-charmed baryon is analyzed through the direct channel $\gamma + \gamma \rightarrow \Xi_{bc} + \bar{c} + \bar{b}$ and the resolved channel $\gamma + g \rightarrow \Xi_{bc} + \bar{c} + \bar{b}$ within the NRQCD factorization framework. The rest parts are arranged as follows. In Sec. II, the necessary calculation formulas and technology are provided. The numerical results are presents in Sec. III, involving cross sections, transverse momentum, rapidity, angular, and the invariant mass distributions. In the end, Sec. IV is reserved for a brief summary.

II. CALCULATION TECHNOLOGY

In the factorization framework of NRQCD, the differential cross section for the photo-production of Ξ_{bc} can be factorized into

$$\begin{aligned} d\sigma(e^+e^- \rightarrow e^+e^- + \Xi_{bc} + \bar{c} + \bar{b}) &= \int dx_1 f_{\gamma/e}(x_1) \int dx_2 f_{\gamma/e}(x_2) \\ &\times \sum_{i,j} \int dx_i f_{i/\gamma}(x_i) \int dx_j f_{j/\gamma}(x_j) \times \sum_n d\hat{\sigma}(ij \rightarrow \langle bc \rangle[n] + \bar{c} + \bar{b}) \langle \mathcal{O}^{\Xi_{bc}}[n] \rangle, \end{aligned} \quad (1)$$

in which, the energy spectrum of the LBS photon $f_{\gamma/e}(x)$ can be described by Ginzburg et al. [66],

$$f_{\gamma/e}(x) = \frac{1}{N} \left(1 - x + \frac{1}{1-x} - \frac{4x}{x_m(1-x)} + \frac{4x^2}{x_m^2(1-x)^2} \right), \quad (2)$$

where $x = E_\gamma/E_e$ represents the energy fraction of the LBS photon emitted from the initial electron or positron, and the normalization factor N is

$$N = \left(1 - \frac{4}{x_m} - \frac{8}{x_m^2} \right) \log(1+x_m) + \frac{1}{2} + \frac{8}{x_m} - \frac{1}{2(1+x_m)^2}, \quad (3)$$

with $x_m = 4E_e E_l \cos^2 \frac{\theta}{2}$ (E_e and E_l represent the energies of the incident electron and laser beams, respectively, and the angle between them denotes as θ). The range of energy fraction x for the LBS photon is constrained by [67]

$$0 \leq x \leq \frac{x_m}{1+x_m} (x_m \approx 4.83). \quad (4)$$

For two different initial sub-processes, $\gamma + \gamma$ and $\gamma + g$, the Glück-Reya-Schienbein (GRS) distribution function $f_{i/\gamma}$ ($i = \gamma, g, u, d, s$) of parton i in the photon [68] is needed, and $f_{\gamma/\gamma}(x) = \delta(1-x)$ is for the direct photoproduction process $\gamma + \gamma$. The differential partonic cross-section $d\hat{\sigma}(ij \rightarrow \langle bc \rangle[n] + \bar{c} + \bar{b})$ can be evaluated perturbatively for $\gamma + \gamma$ and $\gamma + g$ sub-processes. For the partonic processes at leading order in $\mathcal{O}(\alpha_s^3)$, there are 20 Feynman diagrams for $\gamma + \gamma \rightarrow \Xi_{bc} + \bar{c} + \bar{b}$ and 24 diagrams for $\gamma + g \rightarrow \Xi_{bc} + \bar{c} + \bar{b}$. Twelve typical Feynman diagrams for $\gamma(p_1) + g(p_2) \rightarrow \langle bc \rangle[n](q_1) + \bar{c}(q_2) + \bar{b}(q_3)$ are shown in Fig. 1, and another twelve can be obtained by interchanging the initial photon and gluon lines. The Feynman diagrams for $\gamma(p_1) + \gamma(p_2) \rightarrow \langle bc \rangle[n](q_1) + \bar{c}(q_2) + \bar{b}(q_3)$ can be found in earlier study [59], and they will not be shown here.

The differential cross section $d\hat{\sigma}(ij \rightarrow \langle bc \rangle[n] + \bar{c} + \bar{b})$ can be rewritten as

$$d\hat{\sigma}(ij \rightarrow \langle bc \rangle[n] + \bar{c} + \bar{b}) = \frac{1}{4\sqrt{(p_1 \cdot p_2)^2 - m_e^4}} \sum |M[n]|^2 d\Phi_3, \quad (5)$$

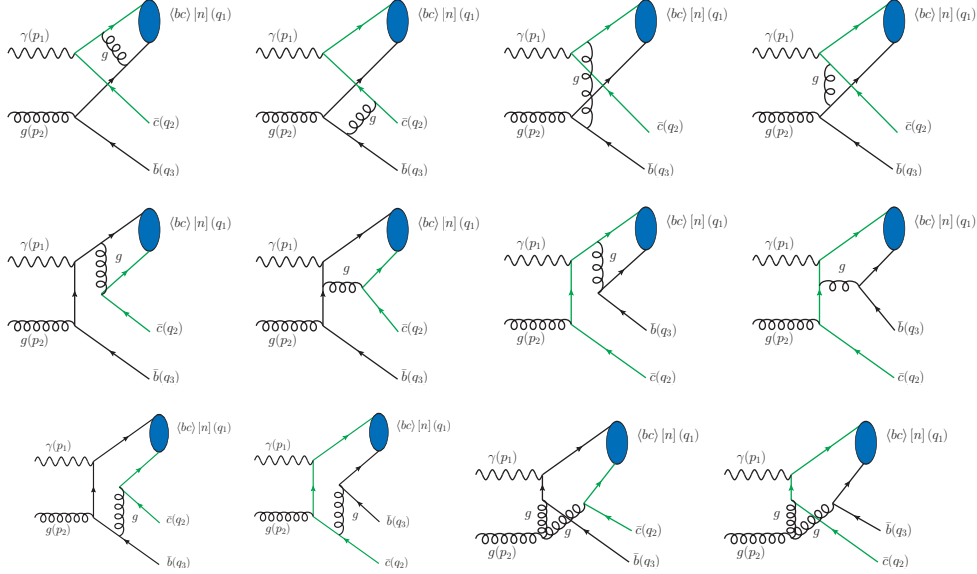


Figure 1. Twelve typical Feynman diagrams for the photoproduction of Ξ_{bc} through the intermediate subprocess $\gamma + g \rightarrow \langle bc \rangle[n] + \bar{c} + \bar{b}$, another twelve can be obtained by interchanging the initial photon and gluon lines.

in which $\overline{\sum}$ is the average over the spins of the initial states and the sum over colors and spins of the final states, $d\Phi_3$ is the three-body phase space. For the production of bottom-charmed baryons Ξ_{bc} , the spin and color quantum number $[n]$ of $\langle bc \rangle$ -diquark configurations can be $\langle bc \rangle[1S_0]_{\bar{3}/6}$, $\langle bc \rangle[3S_1]_{\bar{3}/6}$, $\langle bc \rangle[1P_1]_{\bar{3}/6}$ or $\langle bc \rangle[3P_J]_{\bar{3}/6}$. To obtain the amplitude $\mathcal{M}[n]$, two necessary actions need to be applied. First, the charge conjugation matrix $C = -i\gamma^2\gamma^0$ needs to be applied to reverse the $c \sim \bar{c}$ fermion chain (green line in Fig. 1). It has been proved that with the charge conjugation matrix C , the amplitude for the production of $b(q_{11})c(q_{12}) + \bar{c}(q_2) + \bar{b}(q_3)$ can be related to the amplitude of $b(q_{11})\bar{c}(q_{12}) + c(q_2) + \bar{b}(q_3)$ with an additional factor $(-1)^{(n+1)}$ (n is the number of vector vertices in the fermion chain) [35, 38, 59]. Here $q_{11} = \frac{m_b}{M_{bc}}q_1 + q$ and $q_{12} = \frac{m_c}{M_{bc}}q_1 - q$ are the momenta of b and c constituent quarks with q_1 being the momentum of the $\langle bc \rangle$ -diquark. In the framework of NRQCD, the relative momentum q between two constituent quarks is very small and can be set to be zero in the amplitude of S -wave diquark. The mass of diquark $M_{bc} = m_b + m_c$ is adopted to ensure the gauge invariance of the amplitude. Then the spin projector $\Pi_{q_1}(q)[n]$ is needed to transform the $b(q_{11})\bar{c}(q_{12})$ constituent quarks into bound states $\langle b\bar{c} \rangle(q_1)$ and it takes the form of [69]

$$\Pi_{q_1}(q)[n] = \frac{1}{2\sqrt{M_{bc}}}\varepsilon[n](q_1 + M_{bc}), \quad (6)$$

for $\varepsilon[1S_0] = \gamma^5$ and $\varepsilon[3S_1] = \not{q}$ with the polarization vector ε^β of 3S_1 diquark state. The amplitudes of P -wave Ξ_{bc} can be obtained by the first-derivation of the relative momentum q between two constituent quarks in S -wave amplitude,

$$\mathcal{M}[1P_1] = \varepsilon_\alpha^l(q_1) \frac{d}{dq_\alpha} \mathcal{M}[1S_0]|_{q=0}, \quad (7)$$

$$\mathcal{M}[3P_J] = \varepsilon_{\alpha\beta}^J(q_1) \frac{d}{dq_\alpha} \mathcal{M}^\beta[3S_1]|_{q=0}, \quad (8)$$

in which the relative momentum q is always included in the momenta of the constituent quark of the diquark, q_{11} and q_{12} , and appears in the spin projector Π_{q_1} and propagators.

$\varepsilon_\alpha^l(q_1)$ and $\varepsilon_{\alpha\beta}^J(q_1)$ correspond to the polarization vector and polarization tensor of the spin singlet and spin triplet P -wave states, where J can be 0, 1, or 2. The summations over polarization vector and tensor satisfy [69]

$$\sum_{l_z} \varepsilon_\alpha^l \varepsilon_{\alpha'}^{l*} = \Pi_{\alpha\alpha'} \quad (9)$$

$$\varepsilon_{\alpha\beta}^0 \varepsilon_{\alpha'\beta'}^{0*} = \frac{1}{3} \Pi_{\alpha\beta} \Pi_{\alpha'\beta'} \quad (10)$$

$$\sum_{J_z} \varepsilon_{\alpha\beta}^1 \varepsilon_{\alpha'\beta'}^{1*} = \frac{1}{2} (\Pi_{\alpha\alpha'} \Pi_{\beta\beta'} - \Pi_{\alpha\beta'} \Pi_{\alpha'\beta}) \quad (11)$$

$$\sum_{J_z} \varepsilon_{\alpha\beta}^2 \varepsilon_{\alpha'\beta'}^{2*} = \frac{1}{2} (\Pi_{\alpha\alpha'} \Pi_{\beta\beta'} + \Pi_{\alpha\beta'} \Pi_{\alpha'\beta}) - \frac{1}{3} \Pi_{\alpha\beta} \Pi_{\alpha'\beta'}, \quad (12)$$

with the definition $\Pi_{\alpha\beta} = -g_{\alpha\beta} + \frac{q_{1\alpha}q_{1\beta}}{M_{bc}^2}$.

The color factor $\mathcal{C}_{ij,k}$ for all the Feynman diagrams has been extracted from the amplitude and it satisfies $\mathcal{C}_{ij,k} = \mathcal{N} \times \sum_{a,m,n} (T^a)_{mi} (T^a)_{nj} \times G_{mnk}$, where the normalization constant $\mathcal{N} = \sqrt{1/2}$, i, j, m, n are the color indices of four heavy quarks, k denotes the color index of the diquark, and G_{mnk} corresponds to either the antisymmetric function ε_{mnk} for the color anti-triplet state, or the symmetric function f_{mnk} for the sextuplet state, they satisfy

$$\varepsilon_{mnk} \varepsilon_{m'n'k} = \delta_{mm'} \delta_{nn'} - \delta_{mn'} \delta_{nm'}, \quad (13)$$

$$f_{mnk} f_{m'n'k} = \delta_{mm'} \delta_{nn'} + \delta_{mn'} \delta_{nm'}. \quad (14)$$

Through the above pQCD calculations, we can obtain the short-distance coefficients for the production of intermediate $\langle bc \rangle$ -diquark state. The next step is the crucial hadronization process of the diquark state transitioning to the Ξ_{bc} baryons through the strong interaction.

The long-distance matrix element (LDME) $\langle \mathcal{O}^{\Xi_{bc}}[n] \rangle$ in Eq. 1 can be described by $h_{\bar{3}}$ and h_6 for anti-triplet and sextuplet states, which is non-perturbative and accompanied by significant theoretical uncertainty. Typically, $h_{\bar{3}}$ can be obtained by the potential model and approximately correlated to the Schrödinger wave function at the origin for S -wave diquark, and the first-derivative wave function at the origin for P -wave states [20, 70–73], which can be naturally connected to the (derivative) radial wave function at the origin, i.e.,

$$h_{\bar{3}}[S] \simeq |\Psi_{bc}(0)|^2 = \frac{1}{4\pi} |R_{bc}(0)|^2, \quad (15)$$

$$h_{\bar{3}}[P] \simeq |\Psi'_{bc}(0)|^2 = \frac{3}{4\pi} |R'_{bc}(0)|^2. \quad (16)$$

As for h_6 , there is no such clear correlation, however, according to the power counting rule of NRQCD, both h_6 and $h_{\bar{3}}$ are assigned equivalent orders [65]. Therefore, we adopt $h_6 = h_{\bar{3}}$ in the subsequent calculations to estimate the contribution of color sextuplet. And the uncertainty caused by h_6 will be discussed at next section in detail.

III. NUMERICAL RESULTS

In the numerical calculation, the input parameters are listed below [20, 74]

$$|R_{bc}(0)| = 0.722 \text{ GeV}^{3/2}, \quad |R'_{bc}(0)| = 0.200 \text{ GeV}^{5/2}, \\ m_b = 5.1 \text{ GeV}, \quad m_c = 1.8 \text{ GeV}, \quad M_{bc} = m_b + m_c. \quad (17)$$

$$G_F = 1.1663787 \times 10^{-5}, \quad \mu = \sqrt{M_{\Xi_{bc}}^2 + p_T^2}, \quad (18)$$

where $|R_{bc}(0)|$ and $|R'_{bc}(0)|$ are evaluated under the K²O potential motivated by QCD with a three-loop function [75]. The renormalization scale is typically taken as the transverse mass of Ξ_{bc} with the transverse momentum p_T . Based on that, the strong coupling constant α_s can be obtained with the one-loop running formulation.

At ILC and CLIC with the collision energy $\sqrt{s} = 250, 500, 1000 \text{ GeV}$, the cross section of all considered intermediate diquark states are conducted via both photon-photon fusion and photon-gluon fusion, and the results are provided in Tables I-II. By summing up all the considered intermediate states, we obtained the total contributions of S -wave and P -waves, and the results are listed in Table III. From these three tables, we can see that

- With the increasing of \sqrt{s} , the contribution of each $\langle bc \rangle$ -diquark state decreases via $\gamma + \gamma$ fusion. However, for $\gamma + g$ fusion, the contribution of each $\langle bc \rangle$ -diquark state increases as the energy increases. Based on the comprehensive analysis of the two subprocesses of photoproduction, the total cross-section increases with the increase of collision energy. At $\sqrt{s} = 250 \text{ GeV}$, the contribution of $\gamma + \gamma$ fusion is dominant in the photoproduction process. When the collision energy reaches 500 GeV or higher, the contribution of photon-gluon fusion shows a clearly overwhelming trend.
- Among these diquark states, the contribution of $[{}^3S_1]_{\bar{3}}$ is the largest, accounting for 42.33% (42.45%, and 42.61% (39.21%, 39.31%, and 39.37%) of the total in $\gamma + \gamma$ ($\gamma + g$) fusion when $\sqrt{s} = 250, 500, 1000 \text{ GeV}$. The $[{}^3P_2]_{\bar{3}}$ state dominates the total P -wave state, accounting for 33.69% (33.59% and 33.43%) and 26.54% (26.92% and 27.05%) in $\gamma + \gamma$ and $\gamma + g$ fusion when $\sqrt{s} = 250$ (500 and 1000) GeV, respectively.
- The contribution of S -wave diquark states is significantly larger than that of the P -wave. For the subprocess $\gamma + \gamma$ ($\gamma + g$) fusion when $\sqrt{s} = 250, 500, 1000 \text{ GeV}$, the contribution of the P -wave state is 8.45%, 8.79%, and 9.01% (7.77%, 7.79%, and 7.77%) of that of the S -wave.

Based on the analysis of two subprocesses of photoproduction, the contributions of P -wave state is 7% ~ 9% of the S -wave production. Assuming that at ILC and CLIC with an integrated luminosity of $\mathcal{O}(10^4) \text{ fb}^{-1}$, the produced events of P -wave excited baryons Ξ_{bc} from two subprocess of photoproduction can be approximately 5.21×10^4 (5.75×10^4 , 8.05×10^4) at $\sqrt{s} = 250$ (500, 1000) GeV. Subsequently, the P -wave excited bottom-charmed baryons are likely to decay to the ground state with almost 100% probability, thereby significantly enhancing the production rate of the ground-state Ξ_{bc} baryons.

To reveal more kinematic characteristics for the photoproduction of Ξ_{bc} at ILC and CLIC ($\sqrt{s} = 500 \text{ GeV}$ is selected as a representative), the differential distributions are presented in Fig.2, including the transverse momentum (p_T) and the rapidity (y) of Ξ_{bc} in diquark multi-states, the invariant mass (s_{35} and s_{45}) and the angular ($\cos\theta_{34}$ and $\cos\theta_{35}$) distributions.

Table I. The cross sections σ (in unit: fb) of all considered intermediate diquark states for Ξ_{bc} photoproduction via photon-photon fusion using LBS spectrum at ILC and CLIC with different collision energy \sqrt{s} (GeV).

\sqrt{s}	$\sigma[n]$	$[^1S_0]_{\bar{3}}$	$[^1S_0]_6$	$[^3S_1]_{\bar{3}}$	$[^3S_1]_6$	$[^1P_1]_{\bar{3}}$	$[^1P_1]_6$	$[^3P_0]_{\bar{3}}$	$[^3P_0]_6$	$[^3P_1]_{\bar{3}}$	$[^3P_1]_6$	$[^3P_2]_{\bar{3}}$	$[^3P_2]_6$
250	7.90	3.95	17.47	8.73	0.40	0.20	0.33	0.17	0.33	0.16	1.08	0.54	
500	3.80	1.90	8.57	4.28	0.21	0.10	0.17	0.08	0.16	0.08	0.55	0.27	
1000	1.61	0.80	3.69	1.85	0.09	0.05	0.07	0.04	0.07	0.04	0.24	0.12	

Table II. The cross sections σ (in unit: fb) of all considered intermediate diquark states for Ξ_{bc} photoproduction via photon-gluon fusion using LBS spectrum at ILC and CLIC with different collision energy \sqrt{s} (GeV).

\sqrt{s}	$\sigma[n]$	$[^1S_0]_{\bar{3}}$	$[^1S_0]_6$	$[^3S_1]_{\bar{3}}$	$[^3S_1]_6$	$[^1P_1]_{\bar{3}}$	$[^1P_1]_6$	$[^3P_0]_{\bar{3}}$	$[^3P_0]_6$	$[^3P_1]_{\bar{3}}$	$[^3P_1]_6$	$[^3P_2]_{\bar{3}}$	$[^3P_2]_6$
250	3.27	2.28	10.90	9.34	0.28	0.28	0.08	0.05	0.16	0.13	0.53	0.49	
500	6.87	4.69	22.37	18.87	0.57	0.56	0.15	0.11	0.35	0.28	1.11	1.00	
1000	12.44	8.40	40.08	33.54	1.03	0.98	0.27	0.19	0.62	0.49	1.98	1.77	

Here the definitions of the invariant mass are $s_{35} = (q_1 + q_3)^2$ and $s_{45} = (q_2 + q_3)^2$, θ_{35} (θ_{45}) is the angle between the momenta q_1 (q_2) and q_3 . Due to the excessive intermediate $\langle bc \rangle$ -diquark states in the two subprocesses of photoproduction and the similar trends of each diquark state in S -wave and P -wave, the contribution of each diquark state in S -wave and P -wave is summed when presenting the differential distributions. To analyze the overall distribution, the contributions of S -wave and P -wave are summed up and labeled as Total.

Six different distributions all show that the contribution of S -wave is clearly dominant throughout the whole region compared with the P -wave of each sub-process. The distribution of transverse momentum p_T in Fig.2 reveals that both in S -wave and P -wave, the photoproduction of Ξ_{bc} through $\gamma + g$ fusion is larger than that via photon-photon fusion channel in the region of small p_T , however when p_T is greater than about 40 GeV, a significant reverse increase occurs. The overall trend of total S -wave and P -waves shows a downward trend, and there are significantly more events in small p_T region. For the rapidity distribution for the photoproduction, two subprocesses are concentrated within the range of [-4.2, +4.2], and the curve of $\gamma + g$ has a steeper slope, while that of $\gamma + \gamma$ is more grad-

Table III. The total cross sections σ (in unit: fb) for Ξ_{bc} photoproduction via photon-photon and photon-gluon fusion using LBS spectrum at ILC and CLIC with different collision energy \sqrt{s} (GeV).

\sqrt{s}	$\gamma + \gamma$			$\gamma + g$			Total
	S -wave	P -wave	total	S -wave	P -wave	total	
250	38.05	3.21	41.26	25.79	2.00	27.79	69.05
500	18.55	1.63	20.18	52.80	4.12	56.92	77.10
1000	7.95	0.72	8.66	94.45	7.33	101.79	110.45

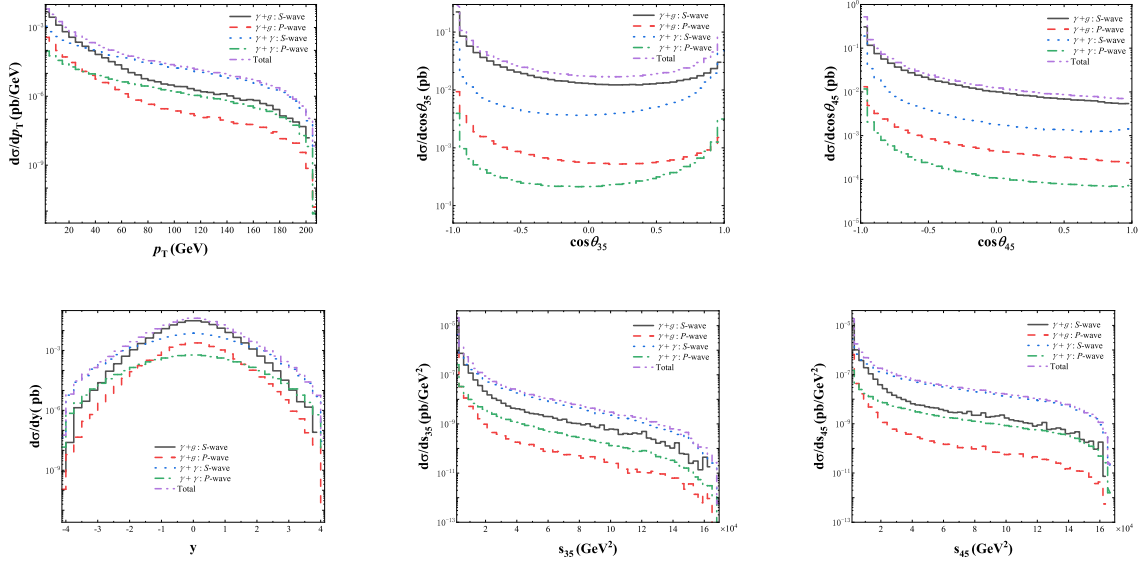


Figure 2. Kinematic distributions for the photoproduction of Ξ_{bc} at ILC and CLIC with $\sqrt{s} = 500$ GeV.

ual. It can be seen from the angular distributions $\cos\theta_{45}$ that when the angle is π , that is, when the two heavy antiquarks move back-to-back, the contribution is the greatest. $\cos\theta_{35}$ indicates that the contribution is significant when the angle is 0 or π , meaning that the bottom-charmed baryon is most likely to move parallel to the two heavy antiquarks. The same conclusion has also been evident in the distributions of the invariant mass s_{35} and s_{45} .

To be mentioned that in the hadronization of the bottom-charmed baryons, it will be accompanied by a large non-perturbative effect, which brings a large theoretical uncertainty. Especially for the color sextuplet baryons, there is no clear correlation with the wave functions. According to the “one-gluon-exchange” interaction in the diquark state, the contribution of the color sextuplet shall be suppressed by q^2 than color anti-triplet, or too small to be ignored [35, 65], the total events of Ξ_{bc} baryon are decreased accordingly. Thus the theoretical uncertainty caused by the transition probability h_6 for the photoproduction of Ξ_{bc} at ILC and CLIC are presented in Table IV with $h_6 = 0$, $q^2 h_{\bar{3}}$ ($q^2 = 0.1 - 0.3$), or $h_{\bar{3}}$. As can be seen from Table IV, the total events of Ξ_{bc} will be reduced by up to 38.12%, 41.80%, and 43.69% for different collision energies $\sqrt{s} = 250, 500, 1000$ GeV, and the order of magnitude for the photoproduction of Ξ_{bc} will not be affected and the total events of bottom-charmed baryons remain significant.

IV. SUMMARY

Within the factorization framework of NRQCD, the photoproduction of ground and excited Ξ_{bc} are investigated at ILC and CLIC with three different collision energies $\sqrt{s} = 250, 500, 1000$ GeV, respectively. The direct and resolved photoproduction channels are both taken into account with intermediate $\langle bc \rangle$ -diquark state, i.e., $\gamma + \gamma \rightarrow \langle bc \rangle[n] + \bar{c} + \bar{b} \rightarrow \Xi_{bc} + \bar{c} + \bar{b}$ and $\gamma + g \rightarrow \langle bc \rangle[n] + \bar{c} + \bar{b} \rightarrow \Xi_{bc} + \bar{c} + \bar{b}$. Twelve configurations of $\langle bc \rangle$ -diquark states can be $(bc)[^1S_0]_{\bar{3}/6}$, $(bc)[^3S_1]_{\bar{3}/6}$, $(bc)[^1P_1]_{\bar{3}/6}$, $(bc)[^3P_0]_{\bar{3}/6}$, $(bc)[^3P_1]_{\bar{3}/6}$, and

Table IV. The theoretical uncertainty of the total cross sections σ (in unit: fb) for the photoproduction of Ξ_{bc} caused by the transition probability $h_6 = 0$, $q^2 h_{\bar{3}}$ ($q^2 = 0.1 - 0.3$), or $h_{\bar{3}}$ at ILC and CLIC with different collision energy \sqrt{s} (GeV).

\sqrt{s}	$h_6 = 0$			$h_6 = q^2 h_{\bar{3}}$			$h_6 = h_{\bar{3}}$		
	$\gamma + \gamma$	$\gamma + g$	Total	$\gamma + \gamma$	$\gamma + g$	Total	$\gamma + \gamma$	$\gamma + g$	Total
250	27.51	15.22	42.73	28.88-31.63	16.47-18.99	45.35-50.62	41.26	27.79	69.05
500	13.45	31.42	44.87	14.13-15.47	33.97-39.07	48.10-54.54	20.18	56.92	77.10
1000	5.77	56.42	62.19	6.06-6.64	60.95-70.03	67.01-76.67	8.66	101.79	110.45

$(bc)[^3P_2]_{\bar{3}/6}$. The cross section of each state has been performed numerical calculation, and the related differential distributions are also presented, including p_T , y , s_{35} , s_{45} , $\cos\theta_{34}$, and $\cos\theta_{35}$ distribution. Finally, the theoretical uncertainty caused by the transition probability $h_6 = 0$, $q^2 h_{\bar{3}}$ ($q^2 = 0.1 - 0.3$), or $h_{\bar{3}}$ has been analyzed for the total cross sections of Ξ_{bc} photoproduction at ILC and CLIC.

The numerical results show that the photoproduction of P -wave Ξ_{bc} is about 7%-9% of that of the S -wave. Assuming that the P -wave excited bottom-charmed baryons are likely to decay to the ground state with almost 100% probability, the produced events of ground-state Ξ_{bc} baryons from two subprocesses of the photoproduction can be approximately 6.91×10^5 , 7.71×10^5 , and 1.10×10^6 at ILC and CLIC with collision energy $\sqrt{s} = 250$, 500, and 1000 GeV, respectively, when the integrated luminosity is $\mathcal{O}(10^4)$ fb $^{-1}$. If the theoretical uncertainty caused by the transition probability h_6 is taken into account, the total number of produced Ξ_{bc} events might decrease by up to 38.12%, 41.80%, and 43.69% for different collision energies $\sqrt{s} = 250$, 500, 1000 GeV, and the overall order of magnitude for the photoproduction of Ξ_{bc} will remain unchanged and the total events of bottom-charmed baryons remain significant.

The differential distributions all emphasize the contribution of S -wave is dominant throughout the whole region compared with the P -wave of each sub-process. The transverse momentum distribution reveals that both in S -wave and P -wave, the photoproduction of Ξ_{bc} through the resolved $\gamma + g$ channel is larger than that via photon-photon fusion in the region of small p_T . The overall trend of total S -wave and P -waves shows a downward trend, and there are significantly more events in small p_T region. For the rapidity distribution for the photoproduction, the curve of $\gamma + g$ has a steeper slope, while that of $\gamma + \gamma$ is more gradual. It can be seen from the angular distributions $\cos\theta_{35}$ and $\cos\theta_{45}$ that the bottom-charmed baryon is most likely to move parallel to the two heavy antiquarks. The same conclusion has also been evident in the distributions of the invariant mass s_{35} and s_{45} .

ACKNOWLEDGMENTS

This work was supported by the National Natural Science Foundation of China (Grants No. 12505106) and by the Natural Science Foundation of Guangxi (No. 2024GXNSFBA010368, No. 2025GXNSFAA069775), this work was also supported by Guangxi Young Elite Scientist Sponsorship Program (No. GXYESS2025005). H.-H. Ma is also supported by the São Paulo

Research Foundation (FAPESP), Brasil. Process Number 2025/01276-7.

- [1] R. Aaij *et al.* [LHCb], “Observation of the doubly charmed baryon Ξ_{cc}^{++} ,” *Phys. Rev. Lett.* **119**, 112001 (2017).
- [2] R. Aaij *et al.* [LHCb], “First Observation of the Doubly Charmed Baryon Decay $\Xi_{cc}^{++} \rightarrow \Xi_c^+ \pi^+$,” *Phys. Rev. Lett.* **121**, 162002 (2018).
- [3] R. Aaij *et al.* [LHCb], “Measurement of the Lifetime of the Doubly Charmed Baryon Ξ_{cc}^{++} ,” *Phys. Rev. Lett.* **121**, 052002 (2018).
- [4] M. Gell-Mann, “A Schematic Model of Baryons and Mesons,” *Phys. Lett.* **8**, 214 (1964).
- [5] G. Zweig, “An SU(3) model for strong interaction symmetry and its breaking, Version 1,” Report No. CERN-TH-401.
- [6] G. Zweig, “An SU(3) model for strong interaction symmetry and its breaking, Version 2,” Report No. CERN-TH-412.
- [7] R. Aaij *et al.* [LHCb], “Search for the doubly heavy baryon Ξ_{bc}^+ decaying to $J/\psi \Xi_c^+$,” *Chin. Phys. C* **47**, 093001 (2023).
- [8] R. Aaij *et al.* [LHCb], “Search for the doubly heavy Ξ_{bc}^0 baryon via decays to $D^0 p K^-$,” *JHEP* **11**, 095 (2020).
- [9] R. Aaij *et al.* [LHCb], “Search for the doubly heavy baryons Ω_{bc}^0 and Ξ_{bc}^0 decaying to $\Lambda_c^+ \pi^-$ and $\Xi_c^+ \pi^-$,” *Chin. Phys. C* **45**, 093002 (2021).
- [10] S. S. Gershtein, V. V. Kiselev, A. K. Likhoded and A. I. Onishchenko, “Spectroscopy of doubly heavy baryons,” *Phys. Rev. D* **62**, 054021 (2000).
- [11] J. Oudichhya, K. Gandhi and A. Kumar Rai, “Mass spectra of Ξ_{cc} , Ξ_{bc} , Ω_{cc} , and Ω_{bc} baryons in Regge phenomenology,” *Phys. Scripta* **97**, 054001 (2022).
- [12] Q. Qin, Y. J. Shi, W. Wang, G. H. Yang, F. S. Yu and R. Zhu, “Inclusive approach to hunt for the beauty-charmed baryons Ξ_{bc} ,” *Phys. Rev. D* **105**, L031902 (2022).
- [13] Y. J. Shi, W. Wang and Z. X. Zhao, “QCD Sum Rules Analysis of Weak Decays of Doubly-Heavy Baryons,” *Eur. Phys. J. C* **80**, 568 (2020).
- [14] Z. Ghalenovi, C. P. Shen and M. Moazzen Sorkhi, “Mass spectra and semileptonic decays of doubly heavy Ξ and Ω baryons,” *Phys. Lett. B* **834**, 137405 (2022).
- [15] N. Mathur, M. Padmanath and S. Mondal, “Precise predictions of charmed-bottom hadrons from lattice QCD,” *Phys. Rev. Lett.* **121**, 202002 (2018).
- [16] N. Mohajery, N. Salehi and H. Hassanabadi, “A New Model for Calculating the Ground and Excited States Masses Spectra of Doubly Heavy Ξ Baryons,” *Adv. High Energy Phys.* **2018**, 1326438 (2018).
- [17] Y. Song, D. Jia, W. Zhang and A. Hosaka, “Low-lying doubly heavy baryons: Regge relation and mass scaling,” *Eur. Phys. J. C* **83**, 1 (2023).
- [18] G. H. Yang, E. P. Liang, Q. Qin and K. K. Shao, “Inclusive weak-annihilation decays and lifetimes of beauty-charmed baryons,” *Phys. Rev. D* **106**, 093013 (2022).
- [19] Q. F. Song, Q. F. Lü and A. Hosaka, “Bottom-charmed baryons in a nonrelativistic quark model,” *Eur. Phys. J. C* **84**, 89 (2024).
- [20] S. P. Baranov, “On the production of doubly flavored baryons in pp, ep and gamma gamma collisions,” *Phys. Rev. D* **54**, 3228-3236 (1996).
- [21] G. Chen, X. G. Wu, J. W. Zhang, H. Y. Han and H. B. Fu, “Hadronic production of Ξ_{cc} at a fixed-target experiment at the LHC,” *Phys. Rev. D* **89**, 074020 (2014).

- [22] G. Chen, X. G. Wu and S. Xu, “Impacts of the intrinsic charm content of the proton on the Ξ_{cc} hadroproduction at a fixed target experiment at the LHC,” *Phys. Rev. D* **100**, 054022 (2019).
- [23] A. P. Martynenko and A. M. Trunin, “Pair double heavy diquark production in high energy proton–proton collisions,” *Eur. Phys. J. C* **75**, 138 (2015).
- [24] S. Koshkarev, “Production of the Doubly Heavy Baryons, B_c Meson and the All-charm Tetraquark at AFTER@LHC with Double Intrinsic Heavy Mechanism,” *Acta Phys. Polon. B* **48**, 163 (2017).
- [25] S. Koshkarev and V. Anikeev, “Production of the doubly charmed baryons at the SELEX experiment – The double intrinsic charm approach,” *Phys. Lett. B* **765**, 171-174 (2017).
- [26] S. Groote and S. Koshkarev, “Production of doubly charmed baryons nearly at rest,” *Eur. Phys. J. C* **77**, 509 (2017).
- [27] A. V. Berezhnoy, A. K. Likhoded and A. V. Luchinsky, “Doubly heavy baryons at the LHC,” *Phys. Rev. D* **98**, 113004 (2018).
- [28] S. J. Brodsky, S. Groote and S. Koshkarev, “Resolving the SELEX–LHCb double-charm baryon conflict: the impact of intrinsic heavy-quark hadroproduction and supersymmetric light-front holographic QCD,” *Eur. Phys. J. C* **78**, 483 (2018).
- [29] X. G. Wu, “A new search for the doubly charmed baryon Ξ_{cc}^+ at the LHC,” *Sci. China Phys. Mech. Astron.* **63**, 221063 (2020).
- [30] C. H. Chang, J. X. Wang and X. G. Wu, “GENXICC: A Generator for hadronic production of the double heavy baryons Ξ_{cc} , Ξ_{bc} and Ξ_{bb} ,” *Comput. Phys. Commun.* **177**, 467 (2007).
- [31] C. H. Chang, J. X. Wang and X. G. Wu, “GENXICC2.0: An Upgraded Version of the Generator for Hadronic Production of Double Heavy Baryons Ξ_{cc} , Ξ_{bc} and Ξ_{bb} ,” *Comput. Phys. Commun.* **181**, 1144 (2010).
- [32] Z. J. Yang, P. F. Zhang and Y. J. Zheng, “Doubly Heavy Baryon Production in e^+e^- Annihilation,” *Chin. Phys. Lett.* **31**, 051301 (2014).
- [33] J. Jiang, X. G. Wu, Q. L. Liao, X. C. Zheng and Z. Y. Fang, “Doubly Heavy Baryon Production at A High Luminosity e^+e^- Collider,” *Phys. Rev. D* **86**, 054021 (2012).
- [34] J. Jiang, X. G. Wu, S. M. Wang, J. W. Zhang and Z. Y. Fang, “A Further Study on the Doubly Heavy Baryon Production around the Z^0 Peak at A High Luminosity e^+e^- Collider,” *Phys. Rev. D* **87**, 054027 (2013).
- [35] X. C. Zheng, C. H. Chang and Z. Pan, “Production of doubly heavy-flavored hadrons at e^+e^- colliders,” *Phys. Rev. D* **93**, 034019 (2016).
- [36] Z. J. Yang and X. X. Zhao, “The Production of Ξ_{bb} at Photon Collider,” *Chin. Phys. Lett.* **31**, 091301 (2014).
- [37] G. Chen, X. G. Wu, Z. Sun, Y. Ma and H. B. Fu, “Photoproduction of doubly heavy baryon at the ILC,” *JHEP* **12**, 018 (2014).
- [38] X. J. Zhan, X. G. Wu and X. C. Zheng, “Photoproduction of doubly heavy baryons at future e^+e^- colliders,” *Phys. Rev. D* **108**, 074030 (2023).
- [39] H. Y. Bi, R. Y. Zhang, X. G. Wu, W. G. Ma, X. Z. Li and S. Owusu, “Photoproduction of doubly heavy baryon at the LHeC,” *Phys. Rev. D* **95**, 074020 (2017).
- [40] Z. Sun and X. G. Wu, “The production of the doubly charmed baryon in deeply inelastic ep scattering at the Large Hadron Electron Collider,” *JHEP* **07**, 034 (2020).
- [41] G. Chen, C. H. Chang and X. G. Wu, “Hadronic production of the doubly charmed baryon via the proton–nucleus and the nucleus–nucleus collisions at the RHIC and LHC,” *Eur. Phys.*

J. C **78**, 801 (2018).

[42] J. J. Niu, L. Guo, H. H. Ma, X. G. Wu and X. C. Zheng, “Production of semi-inclusive doubly heavy baryons via top-quark decays,” Phys. Rev. D **98**, 094021 (2018).

[43] J. J. Niu, L. Guo, H. H. Ma and X. G. Wu, “Production of doubly heavy baryons via Higgs boson decays,” Eur. Phys. J. C **79**, 339 (2019).

[44] P. H. Zhang, L. Guo, X. C. Zheng and Q. W. Ke, “Excited doubly heavy baryon production via W^+ boson decays,” Phys. Rev. D **105**, 034016 (2022).

[45] X. Luo, H. B. Fu and H. J. Tian, “Investigation of Z-boson decay into and baryons within the NRQCD factorization approach*,” Chin. Phys. C **47**, 053102 (2023).

[46] A. V. Berezhnoy, I. N. Belov and A. K. Likhoded, “Production of doubly charmed baryons with the excited heavy diquark at LHC,” Int. J. Mod. Phys. A **34**, 1950038 (2019).

[47] H. H. Ma, J. J. Niu and X. C. Zheng, “Excited doubly heavy baryons production via top-quark decays,” Phys. Rev. D **107**, 014006 (2023).

[48] X. J. Zhan, X. G. Wu and X. C. Zheng, “Photoproduction of P-wave doubly charmed baryon at future e^+e^- collider,” JHEP **11**, 029 (2023).

[49] A. V. Berezhnoy, V. V. Kiselev and A. K. Likhoded, “Photonic production of S- and P wave B/c states and doubly heavy baryons,” Z. Phys. A **356**, 89 (1996).

[50] M. Klasen, B. A. Kniehl, L. N. Mihaila and M. Steinhauser, “Evidence for color octet mechanism from CERN LEP-2 $\gamma\gamma \rightarrow J/\psi + X$ data,” Phys. Rev. Lett. **89**, 032001 (2002).

[51] S. Frixione, M. L. Mangano, P. Nason and G. Ridolfi, “Improving the Weizsäcker-Williams approximation in electron-proton collisions,” Phys. Lett. B **319**, 339 (1993).

[52] A. Djouadi *et al.* [ILC], “International Linear Collider Reference Design Report Volume 2: Physics at the ILC,” [arXiv:0709.1893 [hep-ph]].

[53] P. N. Burrows *et al.* [CLICdp and CLIC], “The Compact Linear Collider (CLIC) - 2018 Summary Report,” CERN Yellow Rep. Monogr. **2**, 1 (2018).

[54] J. Jiang, S. Y. Li, X. Liang, Y. R. Liu, Z. G. Si and Z. J. Yang, “Production of doubly charmed tetraquark Tcc via photon-photon fusion at electron-positron colliders,” Phys. Lett. B **866**, 139543 (2025).

[55] A. Abada *et al.* [FCC], “FCC-ee: The Lepton Collider: Future Circular Collider Conceptual Design Report Volume 2,” Eur. Phys. J. ST **228**, 261 (2019).

[56] [CEPC Study Group], “CEPC Conceptual Design Report: Volume 1 - Accelerator,” [arXiv:1809.00285 [physics.acc-ph]].

[57] J. B. Guimaraes da Costa *et al.* [CEPC Study Group], “CEPC Conceptual Design Report: Volume 2 - Physics & Detector,” [arXiv:1811.10545 [hep-ex]].

[58] J. Erler, S. Heinemeyer, W. Hollik, G. Weiglein and P. M. Zerwas, “Physics impact of GigaZ,” Phys. Lett. B **486**, 125 (2000).

[59] H. H. Ma, J. J. Niu and L. Guo, “Further study on excited $\Xi_{QQ'}$ via photoproduction at CEPC and FCC-ee,” JHEP **05**, 197 (2025).

[60] J. J. Niu and H. H. Ma, “Photoproduction of doubly charmed tetraquark Tcc via photon-gluon fusion at ILC and CLIC,” Phys. Rev. D **112**, 054002 (2025).

[61] R. Li and K. T. Chao, “Photoproduction of J/ψ in association with a $c\bar{c}$ pair,” Phys. Rev. D **79**, 114020 (2009).

[62] X. J. Zhan, X. G. Wu and X. C. Zheng, “Inclusive J/ψ photoproduction at the ILC within the framework of non-relativistic QCD,” JHEP **09**, 050 (2022).

[63] X. J. Zhan, X. G. Wu and X. C. Zheng, “Photoproduction of the Bc meson at future e^+e^- colliders,” Phys. Rev. D **106**, 094036 (2022).

- [64] G. T. Bodwin, E. Braaten and G. P. Lepage, “Rigorous QCD analysis of inclusive annihilation and production of heavy quarkonium,” *Phys. Rev. D* **51**, 1125 (1995) [erratum: *Phys. Rev. D* **55**, 5853 (1997)].
- [65] J. P. Ma and Z. G. Si, “Factorization approach for inclusive production of doubly heavy baryon,” *Phys. Lett. B* **568**, 135 (2003).
- [66] I. F. Ginzburg, G. L. Kotkin, V. G. Serbo and V. I. Telnov, “Colliding gamma e and gamma gamma Beams Based on the Single Pass Accelerators (of Vlepp Type),” *Nucl. Instrum. Meth.* **205**, 47 (1983).
- [67] V. I. Telnov, “Problems of Obtaining $\gamma\gamma$ and $\gamma\epsilon$ Colliding Beams at Linear Colliders,” *Nucl. Instrum. Meth. A* **294**, 72 (1990).
- [68] M. Gluck, E. Reya and I. Schienbein, “Radiatively generated parton distributions of real and virtual photons,” *Phys. Rev. D* **60**, 054019 (1999) [erratum: *Phys. Rev. D* **62**, 019902 (2000)].
- [69] A. Petrelli, M. Cacciari, M. Greco, F. Maltoni and M. L. Mangano, “NLO production and decay of quarkonium,” *Nucl. Phys. B* **514**, 245 (1998).
- [70] A. F. Falk, M. E. Luke, M. J. Savage and M. B. Wise, “Heavy quark fragmentation to baryons containing two heavy quarks,” *Phys. Rev. D* **49**, 555 (1994).
- [71] V. V. Kiselev, A. K. Likhoded and M. V. Shevlyagin, “Double charmed baryon production at B factory,” *Phys. Lett. B* **332**, 411 (1994).
- [72] E. Bagan, H. G. Dosch, P. Gosdzinsky, S. Narison and J. M. Richard, “Hadrons with charm and beauty,” *Z. Phys. C* **64**, 57 (1994).
- [73] A. V. Berezhnoy, V. V. Kiselev, A. K. Likhoded and A. I. Onishchenko, “Doubly charmed baryon production in hadronic experiments,” *Phys. Rev. D* **57**, 4385 (1998).
- [74] S. Navas *et al.* [Particle Data Group], “Review of particle physics,” *Phys. Rev. D* **110**, 030001 (2024).
- [75] V. V. Kiselev, A. K. Likhoded, O. N. Pakhomova and V. A. Saleev, “Mass spectra of doubly heavy Omega QQ' baryons,” *Phys. Rev. D* **66**, 034030 (2002).